electronics

MDPI

Article

An Intelligent Robust Operator-Based Sliding Mode Control for Trajectory Tracking of Nonlinear Uncertain Systems

Qiang Zhang [1], Ping Liu [2,*], Quan Deng [3], Angxin Tong [1] and Jürgen Pannek [4]

[1] School of Intelligent Engineering, Zhengzhou University of Aeronautics, Zhengzhou 450046, China
[2] Zhongyuan-Petersburg Aviation College, Zhongyuan University of Technology, Zhengzhou 451191, China
[3] BIBA Bremer Institut für Produktion und Logistik GmbH, Faculty of Production Engineering, University of Bremen, 28359 Bremen, Germany
[4] Faculty of Mechanical Engineering, Technische Universität Braunschweig, 38106 Braunschweig, Germany
* Correspondence: pingliu@zut.edu.cn

Abstract: This paper investigates the problem of trajectory tracking control in the presence of bounded model uncertainty and external disturbance. To cope with this problem, we propose a novel intelligent operator-based sliding mode control scheme for stability guarantee and control performance improvement in the closed-loop system. Firstly, robust stability is guaranteed by using the operator-based robust right coprime factorization method. Secondly, in order to further achieve the asymptotic tracking and enhance the responsiveness to disturbance, a finite-time integral sliding mode control law is designed for fast convergence and non-zero steady-state error in accordance with Lyapunov stability analysis. Lastly, the controller's parameters are automatically adjusted by the proved stabilizing particle swarm optimization with the linear time-varying inertia weight, which significantly saves tuning time with a remarkable performance guarantee. The effectiveness and efficiency of the proposed method are verified on a highly nonlinear ionic polymer metal composite application. The extensive numerical simulations are conducted and the results show that the proposed method is superior to the state-of-the-art methods in terms of tracking accuracy and high robustness against disturbances.

Keywords: intelligent nonlinear control; operator theory; robust right coprime factorization; sliding mode control; particle swarm optimization

Citation: Zhang, Q.; Liu, P.; Deng, Q.; Tong, A.; Pannek, J. An Intelligent Robust Operator-Based Sliding Mode Control for Trajectory Tracking of Nonlinear Uncertain Systems. *Electronics* **2023**, *12*, 3379. https://doi.org/10.3390/electronics12163379

Academic Editor: Mahmut Reyhanoglu

Received: 18 July 2023
Revised: 4 August 2023
Accepted: 6 August 2023
Published: 8 August 2023

1. Introduction

Due to algorithm simplicity, transparency, and reliability, the proportional-integral-derivative (PID) control algorithm has been successfully applied to a wide variety of fields, e.g., manufacturing, robotics, aerospace, and bio-medicine. Although PID was invented more than one hundred years ago, it is still in a leading position and has been employed in more than ninety percent (90%) of industrial controllers [1]. The systems with weak nonlinearity may be treated as linear systems in the vicinity of the operating points and therefore can be dealt with PID control method for satisfactory control performance. Yet, PID may be intractable for highly nonlinear systems in the presence of model uncertainty and unpredictable disturbances. To improve the control performance of traditional PID, its variants such as fuzzy logic PID, fractional-order PID, neural network PID, and adaptive PID with swarm intelligence were developed [2,3].

In recent decades, robust nonlinear control methods have attracted increasing attention and have been rapidly and maturely developed. Robust nonlinear model predictive control (NMPC) is an optimization-based control algorithm that can naturally address complex and nonlinear control problems, especially for multi-input multi-output (MIMO) systems with constraints [4–7]. Yet, the referred non-convex optimization problems in control may drastically aggravate the computational burden and pose a challenge in real-time control. Operator-based robust right coprime factorization (RRCF) is a novel robust control method [8]. The core idea behind the RRCF method is that the system model and bounded model uncertainties can be decomposed as stable operators and then the related robust controllers are designed to meet the Bezout identity along with a Lipschitz inequality condition for robust stability. Due to the strong robustness to model uncertainty and disturbance, RRCF had been successfully applied for a variety of practical applications [9,10], such as multi-variable tracking control for manipulators, job shop scheduling and control in advanced manufacturing, nonlinear vibration control for an aircraft vertical tail, nonlinear control, and fault detection for a Peltier actuated thermal process.

Besides the robust stability of RRCF, tracking performance is also important. The most of tracking controllers associated with RRCF are in the form of conventional PI-type [9,11,12]. In [13], a fractional-order PID algorithm combined with RRCF was applied for a complex spiral heat exchanger plant with uncertainties. Due to insensitivity and robustness to disturbances, remarkable computational simplicity, and rapid convergence, sliding mode control (SMC) as a popular robust control algorithm had attracted considerable attention for the disturbed nonlinear systems [14]. In [15], the authors adopted a terminal sliding mode control based on the RRCF method for the tracking performance improvement of wireless power transfer systems with uncertainties. In [16], an integral sliding mode control (ISMC) in conjunction with the RRCF method was used for tracking the soft actuator with a time-varying radius. However, the tracking controllers' parameters are manually adjusted based on the trial-and-error method, which may be very time-consuming and without flexibility and adaptability.

In the tracking control systems, appropriate parameters of controllers play a vital role to enhance the transient and steady-state performance of closed-loop systems. For example, the proportional term in PI control responds to the current error instantaneously while the integral term is responsible for zero steady-state error. The different combinations of parameters have a high impact on the control performance, e.g., overshoot, settling time, and steady-state error. For MPC, the control horizon is a crucial parameter, which determines the computational cost, stability, and closed-loop performance [4]. The coefficient with respect to the discontinuous switching term in SMC results in chattering with a certain magnitude and frequency [17]. Therefore, in order to make the control system smarter, as a subset of the artificial intelligence field, swarm intelligence algorithms including evolutionary algorithms (e.g., genetic algorithm, GA) and metaheuristic algorithms (e.g., particle swarm optimization, PSO) are rapidly emerging and have been successfully applied in the intelligent nonlinear control for parameters optimization [18,19]. For example, the combination of linear quadratic regulator (LQR) and SMC was used for precise pointing of the satellite and its payload while considering the damping disturbances and time-delay effects. The controllers' parameters were optimized by PSO according to the normalized integral square error [20].

In this paper, we propose an intelligent robust nonlinear control method to address the tracking control problem of nonlinear systems in the presence of model uncertainty and external disturbance. To the best of our knowledge, the method of "finite time ISMC-RRCF based PSO" for tracking control was not published in any previous works. The highlights and contributions of this paper can be summarized as follows:

- The model uncertainty is addressed and robust stability can be guaranteed by using the operator-based RRCF method.
- The tracking performance in the presence of model uncertainties and external disturbances can be further guaranteed by the adopted finite-time ISMC-RRCF.
- The parameters of the sliding mode controller are automatically tuned and optimized by the stabilizing PSO to achieve minimal tracking error.
- The proposed control method is evaluated on a highly nonlinear electroactive polymer actuator, and compared to the state-of-the-art methods in terms of tracking performance and robustness through numerical simulations.

The rest of this paper is organized as follows. The operator-based robust right coprime factorization and the finite time integral sliding mode control are presented in Section 2 and Section 3, respectively. Then, the stabilizing particle swarm optimization with linear time-varying inertia weight is introduced for parameter optimization in Section 4. The proposed robust tracking control method is evaluated on a highly nonlinear application with numerical simulations in Section 5. Last, we conclude our work in Section 6.

2. Robust Right Coprime Factorization

In this paper, we consider a class of affine nonlinear systems, which can be expressed as follows:

$$\begin{cases} \dot{x} = f(x) + g(x)u + d \\ y = h(x) \end{cases} \tag{1}$$

where $x = [x_1, x_2, \cdots, x_n]^T \in \mathcal{R}^n$ is the state vector, $f(x)$ and $g(x)$ stand for smooth vector function, $h(x)$ represents the smooth scalar function, $u \in \mathcal{R}$ is the system input, $y \in \mathcal{R}$ is the system output, $d \in \mathcal{R}^n$ represents the unknown but bounded lumped disturbances coming from model uncertainty and external disturbance. In the RRCF control of nonlinear systems, the related concepts and definitions are introduced in [8]. A nonlinear system with input signal $u \in U$ and output signal $y \in Y$ is described as operator P, as shown in Figure 1.

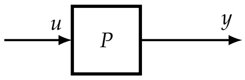

Figure 1. Description of a nonlinear system P.

Here, U and Y are linear input and output spaces. In the control performance analysis, a norm $\|P\|$ is defined as

$$\|P\| := \sup_{x,\tilde{x} \in U \& x \neq \tilde{x}} \frac{\|P(x) - P(\tilde{x})\|_Y}{\|x - \tilde{x}\|_U}.$$

Assuming stable input space $U_s \subseteq U$ and output space $Y_s \subseteq Y$, if $P(U_s) \subseteq Y_s$, then the system is stable. If there exist stable operators $N : W \rightarrow Y$ and $D : W \rightarrow U$ satisfying $P = ND^{-1}$, then we call the system has a right factorization, where D is invertible, and W is called quasistate space, which is linear.

Consider a causal and stabilizable system P. We call P has a right coprime factorization when there exist two stable operators $A : Y \rightarrow U$ and $B : U \rightarrow U$ satisfying the Bezout identity $AN + BD = M$, as shown in Figure 2, where $u \in U$, $w \in W$, $y \in Y$, and M is a unimodular operator.

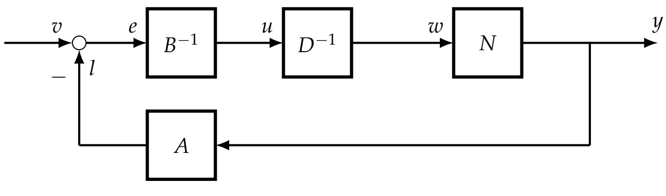

Figure 2. RCF feedback control system.

To include bounded disturbance and uncertainty, ΔN is integrated into operator N as the right factorization of P. Thereafter, the robust feedback control of the disturbed system is formed in Figure 3. Given such a bound disturbed stabilizable system P, if there still exist two stable operators A and B meeting the Bezout identity $A \circ (N + \Delta N) + B \circ D = \tilde{M}$ and $\|(A \circ (N + \Delta N) - A \circ N)M^{-1}\| < 1$, then the system is said to have a robust right coprime factorization, where $\tilde{M}$ is a unimodular operator [9].

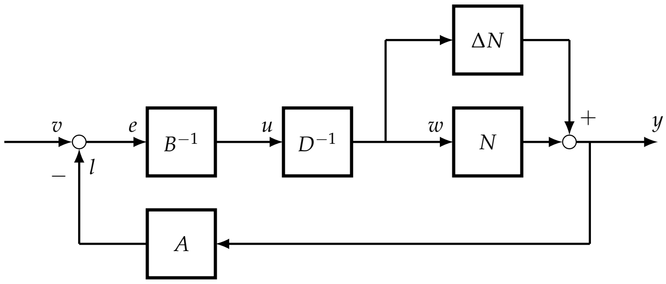

Figure 3. RRCF feedback control system with disturbances.

The above RRCF control scheme is designed for robust stability. In order to achieve the tracking requirement, the following feedback control structure is one popular opportunity [8], as shown in Figure 4. Here, e_T is the error between the reference input signal r and output signal y. C is the tracking controller, which is the main research result that we will introduce in the following sections.

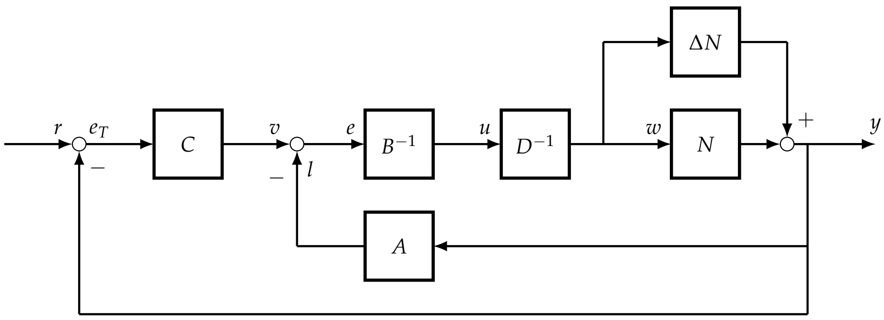

Figure 4. Feedback tracking control of nonlinear systems.

3. Finite Time Integral Sliding Mode Control

For SMC, the first and most important step is the construction of sliding surfaces such as linear switching hyperplanes and nonlinear exponential terminal sliding surfaces. According to the designed sliding manifold, the derived control law, in general, consists of an equivalent control law and a discontinuous switching control law. The latter aims to force the nonlinear state's trajectory onto a pre-specified hyperplane and the former keeps the states on the sliding surface while sliding into the origin. In order to improve tracking performance and reduce steady-state error, we employ an integral sliding mode control (ISMC) associated with the linearized stable differential operator. The designed sliding mode surface is concerned with tracking error and its derivative term and an integral term, i.e.,

$$s(t) = \sum_{i=1}^{n-1} c_i e_{n-1} + e_n + \delta \int_0^{\infty} e_1(t)dt \tag{2}$$

where n represents the system model order, $e_1 = y - y_d$, note that e_1 is equal to e_T in Figure 4, $\dot{e}_i = e_{i+1}, i = 1, \cdots, n-1$, the coefficients $c_i, i = 1, \cdots, n-1$ are set to be positive values such that the roots of polynomial $c_1 + c_2 s + \cdots + c_{n-1} s^{n-2} + s^{n-1}$ lie in the open left half (Hurwitz) plane [21]. To further improve the transient performance with faster convergence and achieve asymptotic stability with finite time convergence in the context of fast and high-precision trajectory tracking control, the ISMC control law can be designed based on the Lyapunov stability analysis. Before introducing the finite time sliding mode controller design, we present a Lemma 1 concerning the finite time stability below.

Lemma 1. *If there exists a positive definite function $V(t)$ such that the differential inequality [22]:*

$$\dot{V}(t) + \varrho V(t) + \Gamma V^{\theta}(t) \leq 0, \forall t > t_0 \tag{3}$$

holds for $t \geq t_0$ *and* $V(t_0) \geq 0$*, then* $V(t)$ *converges to the equilibrium point in finite time with*

$$t_s \leq t_0 + \frac{1}{\varrho(1-\theta)} In \frac{\varrho V^{1-\theta}(t_0) + \Gamma}{\Gamma} \tag{4}$$

where $\varrho > 0, \Gamma > 0, 0 < \theta < 1$.

Now, we choose the Lyapunov function as $V = \frac{1}{2}s^2 > 0$ when $s \neq 0$ and substitute Equation (2) into its derivative below, we obtain that

$$\dot{V} = s\dot{s} = s(\sum_{j=1}^{n-1} c_j \dot{e}_j + y^{(n)} - y_d^{(n)} + \delta \cdot e_1) \tag{5}$$

For the nonlinear systems (1), the relative degree is assumed to the system order. In this case, the control signal u would first appear in $y^{(n)}$. Utilizing Lie derivatives, $y^{(n)}$ is expressed as [23]:

$$y^{(n)} = L_f^n h(x) + L_g L_f^{n-1} h(x) \cdot u + L_{f+gu+d}^{n-1} L_d h(x) + \sum_{\lambda=1}^{n-1} L_{f+gu+d}^{\lambda-1} L_d L_f^{n-\lambda} h(x) \tag{6}$$

We define the sum of the last two terms in (6) concerning the disturbance as d_u and substitute Equation (6) into Equation (5) with the following SMC control law

$$u = \frac{1}{-L_g L_f^{n-1} h(x)} (L_f^n h(x) + \sum_{j=1}^{n-1} c_j \dot{e}_j - y_d^{(n)} + \delta \cdot e_1 + ks + \xi sign(s) + \mu s^{p/q}) \tag{7}$$

where p and q are odd positive integers with $p < q$, $\xi > 0$, $\mu > 0$ and $\delta > 0$. Then, the finite time convergence can be guaranteed with the assumption of $|d_u| < \xi$, i.e.,

$$\begin{aligned}
\dot{V} &= s\dot{s} = s(\sum_{j=1}^{n-1} c_j \dot{e}_j + y^{(n)} - y_d^{(n)} + \delta \cdot e_1) \\
&= s(\sum_{j=1}^{n-1} c_j \dot{e}_j + L_f^n h(x) + L_g L_f^{n-1} h(x) \cdot u + d_u - y_d^{(n)} + \delta \cdot e_1) \\
&= s(-ks - \xi sign(s) - \mu s^{\frac{p}{q}} + d_u) \\
&= -ks^2 - \xi |s| + s \cdot d_u - \mu s^{p/q+1} \\
&\leq -2kV - 2^{\frac{p+q}{2q}} \mu V^{\frac{p+q}{2q}}
\end{aligned} \tag{8}$$

and the finite time can be numerically obtained accordingly, i.e.,

$$t_s < t_0 + \frac{q}{k(q-p)} In(\frac{k s_0^{\frac{q-p}{q}}(t_0)}{\mu} + 1) \tag{9}$$

There are two points that we would like to highlight:

- The high robustness is achieved by the fast switching control actions with $sign(\cdot)$ function but at the expense of chattering which may result in unwanted wear and tear of the actuators and even cause system instability [24]. To suppress or avoid chattering, one straightforward method is using a continuous smoothing function instead of the discontinuous switching control. Another popular method for chattering alleviation is high-order SMC, e.g., super-twisting [25]. In doing so, the control input appeared as the integration of the high-frequency switching terms by making its successive derivative terms to be zero. In this paper, we employ the boundary layer method in which the discontinuous switching term $sign(\cdot)$ in Equation (7) is commonly replaced by a saturation function in the form of

$$sat(s) = \begin{cases} 1, s > \Delta, \\ \kappa s, |s| \leq \Delta, \kappa = \frac{1}{\Delta} \\ -1, s < -\Delta \end{cases} \tag{10}$$

where $\Delta > 0$ represents the thickness of the boundary layer. As a matter of fact, a linear feedback control strategy is adopted inside the given boundary while the switching operation is only applied outside the boundary. It should be noted that a non-zero steady-state error may exist by using the boundary layer method.

- There exist some parameters (e.g., k, ξ, μ, c_j) in the ISMC control law (7), which would definitely influence the closed-loop control performance. These interactional parameters can be automatically tuned by nature-inspired optimization algorithms. However, two problems may arise when using stochastic searching techniques for real-time control, especially for uncertain nonlinear systems. The first is that the repetitive optimization routine may be required for the derived desired parameters with performance guarantee but may fail the systems with unknown model uncertainty. The second is that a local solution rather than the global solution may be found during the searching process, which may result in performance deterioration.

Taking these two points into account, our aim is that the nonlinear systems with unknown but bounded model uncertainty and disturbance are firstly stabilized by the RRCF method, and then the SMC parameters for tracking are optimized by the certified convergent PSO to possibly avoid falling into local optimum.

4. Stabilizing Particle Swarm Optimization

As one of the most popular group intelligence computation techniques, the particle swarm optimization (PSO) algorithm was originally proposed by Kennedy and Eberhart in 1995 [26]. Due to the fast convergence speed, strong global search ability, high solution efficiency, and being derivative free, it has been widely used for solving complex optimization problems in a variety of fields, e.g., mechanical engineering, production engineering, electrical and electronic engineering, automation control systems [27]. The PSO algorithm was inspired by a simulation of a bird swarm's foraging where the "birds—particles" are seeking "food—the best solution" through cooperation and information sharing in the entire searching process. Mathematically, the principle of the basic PSO is realized by dynamically updating the velocity $v_i = [v_{i1}, v_{i2}, \cdots, v_{il}]$ and position $x_i = [x_{i1}, x_{i2}, \cdots, x_{il}]$ for all particles, i.e.,

$$v_i^{G+1} = w^G v_i^G + \chi_1(p_i^G - x_i^G) + \chi_2(p_g^G - x_i^G) \tag{11}$$

$$x_i^{G+1} = x_i^G + v_i^{G+1} \tag{12}$$

where $i = 1, 2, \cdots m$ and $m \in Z^+$ is swarm size, $l \in Z^+$ is dimensionality of search space, $G \in Z^+$ stands for the maximum generation, $\{C_1, C_2\} \in R^+$ are individual and social acceleration coefficients, $\{r_1, r_2\} \in [0, 1]$ are random values for better space exploration, $\chi_1 = C_1 r_1, \chi_2 = C_2 r_2$, p_i^G stands for the best individual solution and p_g^G is the global solution representing the best particle among all the searched particles in the population, $w^G \in R^+$ is inertia weight, representing the capability of global exploration and exploitation of local search. Generally, a large inertia weight facilitates a global search while small ones may tend to local optima. In this case, various inertia weight modification mechanisms have been investigated [28], such as random and adaptive inertia weight, and linear time-varying inertia weight, i.e.,

$$w^G = w_{max} - \frac{w_{max} - w_{min}}{G_{max}} G \tag{13}$$

Remark 1. *Since the PSO algorithm belongs to the probabilistic searching technique, the non-optimal solution may be derived in one generation, which may result in the consequent error for the subsequent iterations, and the stability and convergence of the algorithm itself may be lost due to improper parameter setting. The stability condition concerning the setting of acceleration coefficients and inertia weight was theoretically analyzed by using the Neumann stability criterion associated with the following difference Equation (14), i.e.,*

$$x_i^{G+1} - (1 + w^G - \chi_1 - \chi_2)x_i^G + w^G x_i^{G-1} = \chi_1 p_i^G + \chi_2 p_g^G \tag{14}$$

The PSO algorithm is said to be stable if the χ_1, χ_2 with acceleration coefficient and inertia weight w satisfying the condition below

$$0 \leq (\chi_1 + \chi_2) \leq 2(1 + w^G). \tag{15}$$

In the stable range, the PSO performs better in terms of the accuracy of the solution. We refer to [29] for details.

The procedure of the stabilizing PSO is given in Algorithm 1. Concerning the fitness function in Algorithm 1, there are four common performance assessments with respect to the tracking error, which includes the integral absolute error (IAE $= \int_0^T |e(t)|dt$), the integral square error (ISE $= \int_0^T e(t)^2 dt$), the integral time absolute error (ITAE $= \int_0^T t|e(t)|dt$) and the integral time square error (ITSE $= \int_0^T te(t)^2 dt$). Such objective functions can be selected according to the individual requirements for practical applications. After introducing the related robust control methods with an intelligent computing algorithm, the block diagram of the intelligent ISMC-RRCF-PSO control method is described in Figure 5. Also, the corresponding pseudocode is given in Algorithm 2.

Algorithm 1 Pseudocode of the stabilized PSO algorithm with linear time-varying inertia weight for parameters optimization of sliding mode controller

Require: Swarm size m, maximum number of iterations G_{max}, velocity bound $\mathbb{V} := [v_{min}, v_{max}]$, position bound $\mathbb{X} := [x_{min}, x_{max}]$, acceleration coefficients c_1, c_2, inertia weight bound $\mathbb{W} := [w_{min}, w_{max}]$ and system dimension l.

At $G = 0$, initialize position x_i^G and velocity v_i^G for all particles; initialize PSO parameters considering Equation (15); evaluate fitness function $Fit(x_i^G)$ for all particles and set the local best solution as $p_i^G := x_i^G$ and the global best solution $p_g^G := \{\text{argmin}_{x_i^G \in \mathbb{X}} \ Fit(x_i^G), i = 1, 2, \cdots, m\}$;
for $G = 1 : G_{max}$ **do**
    for $i = 1 : m$ **do**
        Update the linear time-varying inertia weight according to Equation (13) while considering Equation (15);
        Update the particle's velocity and position based on Equations (11) and (12) within the related bounds, respectively;
        If $Fit(x_i^G) < Fit(p_i^{G-1})$, then $p_i^G = x_i^G$; else, $p_i^G = x_i^{G-1}$;
    end for
    Update the global best solution $p_g^G := \{\text{argmin}_{p_i^G \in \mathbb{X}} \ Fit(p_i^G), i = 1, 2, \cdots, m\}$;
    Set $G := G + 1$;
end for

Ensure: The global best solution p_g^G, fitness function value $Fit(p_g^G)$.

Algorithm 2 The procedure of implementing the intelligent ISMC-RRCF-PSO controller

Require: Given the system (1) with bounded disturbances
1: Decompose the plant $P + \Delta P$ into operators $N + \Delta N$ and D^{-1};
2: Design RRCF controllers A and B to meet the Bezout equations for robust stability in the presence of disturbances;
3: Design finite-time ISMC controller for tracking performance improvement with fast convergence;
4: Optimize the parameters of ISMC according to the stabilizing PSO with linear time-varying inertia weight (c.f., Algorithm 1);
5: Apply the ISMC-RRCF control law with the optimized parameters for tracking;
Ensure: Guarantee the tracking accuracy and enhance the robustness in the presence of bounded disturbances.

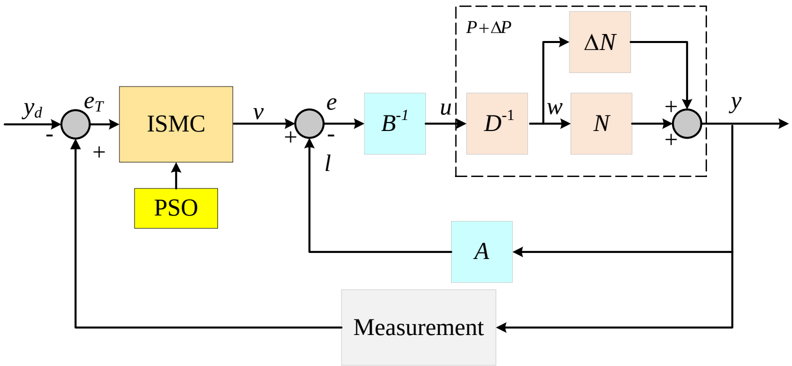

Figure 5. Block diagram of the intelligent ISMC−RRCF control with convergent PSO for the trajectory tracking of nonlinear uncertain systems.

5. Application to Nonlinear Ionic Polymer Metal Composites

Ionic polymer metal composites (IPMC) also called artificial muscle, are one of the most promising electroactive polymer actuators. Due to the characteristics of low driving voltage, small electric consumption, high flexibility, and lightweight, it has been widely applied for a variety of applications such as miniature robots, micro manipulation, and biomedicine devices [30]. Since IPMC belongs to highly nonlinear systems, it may result in avoidable modeling identification errors. In addition to the existing model uncertainty, external disturbance, and control input saturation also have to be considered to achieve the precise and reliable position tracking control of IPMC, which is important to the safe operation of IPMC actuators in the field of biorobotics. Therefore, a practical mathematical model and an effective control method are of great importance to the precise position control. In this paper, we focus on the validation of the proposed robust control algorithm while the elaborate modeling process with respect to IPMC itself can be found in [11]. The established mathematical model is described as

$$\begin{cases} \dot{x} = \dfrac{(x-au)\sqrt{2b(\frac{xe^{-x}}{1-e^{-x}} - In(\frac{xe^{-x}}{1-e^{-x}})-1)}}{SK_e b(R_a+R_c)(1-\frac{1-e^{-x}}{xe^{-x}})\frac{e^{-x}(1-x-e^{-x})}{(1-e^{-x})^2}} + d \\ \\ y = \dfrac{3\alpha_0 K_e\sqrt{2b(\frac{xe^{-x}}{1-e^{-x}} - In(\frac{xe^{-x}}{1-e^{-x}})-1)}}{aY_e H^2} \end{cases} \quad (16)$$

where x is the state variable, y is the curvature output, u is the control input voltage, d is unknown but bounded disturbance including the external disturbance and the uncertainties caused by identifying error of parameters and modeling error of the IPMC, $a = \frac{F}{RT}$, $b = \frac{F^2C^-}{RTK_e}$, $S = WL$ is the surface area of the IPMC, the identified physical parameters are given in Table 1.

Table 1. Parameters of the IPMC model.

Parameter	Notation	Numerical Value
L	The length of IPMC	50 mm
H	The width of IPMC	200 µm
W	The thickness of IPMC	10 mm
T	Absolute temperature	290 K
R_a	Electrodes resistance	18 Ω
R_c	Ion diffusion resistance	60 Ω
Y_e	Equivalent Young modulus	0.056 Gpa
α_0	Coupling constant	0.129 J/C
C^{-1}	Anion concentrations	981 mol/m^2
F	Faraday constant	96,487 C/mol
R	Gas constant	8.3143 J/mol.K
Ke	Effective dielectric constant	1.12×10^{-6} F/m

The shape and the derived bending curvature of IPMC would be changed by an external driving force from the power source, c.f., Figures 6 and 7. The aim is to track the desired curvature and achieve accurate position tracking control in the presence of model uncertainty and disturbance. The reference input signal y_d is set as the time-varying step signal.

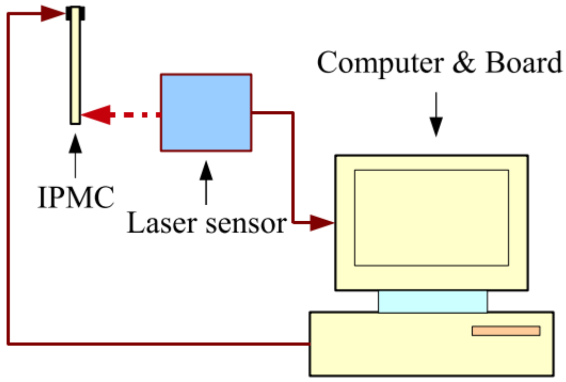

Figure 6. Experimental system schematic illustration.

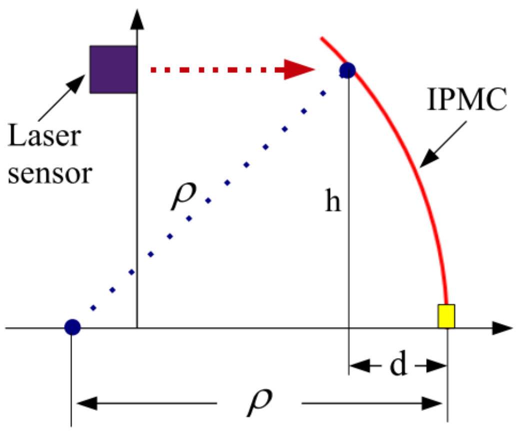

Figure 7. The relationship between curvature output $1/\rho$ with displacement response d.

According to the Algorithm 2 concerning the controller design, the system plant $P + \Delta P$ in Figure 5 is firstly decomposed as $P + \Delta P = (N + \Delta N)D^{-1}$ where N, D, and ΔN are expressed as follows:

$$N(w)(t) = \frac{3\alpha_0 K_e \sqrt{2b(\frac{w(t)e^{-w(t)}}{1-e^{-w(t)}} - ln(\frac{w(t)e^{-w(t)}}{1-e^{-w(t)}}) - 1)}}{aY_e H^2} \tag{17}$$

$$D(w)(t) = \frac{SK_e b(R_a + R_c)\dot{w}(t)(1 - \frac{1-e^{-w(t)}}{w(t)e^{-w(t)}})\frac{e^{-w(t)}(1-e^{-w(t)} - w(t))}{(1-e^{-w(t)})^2}}{a\sqrt{2b(\frac{w(t)e^{-w(t)}}{1-e^{-w(t)}} - ln(\frac{w(t)e^{-w(t)}}{1-e^{-w(t)}}) - 1)}} + \frac{w(t)}{a} \tag{18}$$

$$\Delta N(w)(t) = \Delta\sqrt{(\frac{w(t)e^{-w(t)}}{1-e^{-w(t)}} - ln(\frac{w(t)e^{-w(t)}}{1-e^{-w(t)}}) - 1)} \tag{19}$$

Then, the stable operator controllers A and B are designed as

$$A(y)(t) = -\frac{aSY_e H^2(R_a + R_c)}{3\alpha_0}\dot{y}(t) \tag{20}$$

$$B(u)(t) = au(t) \tag{21}$$

to satisfy the Bezout equations $AN + BD = I$ and $\|(A \circ (N + \Delta N) - A \circ N)\| < 1$, where I is the identity operator and $\|\Delta\| < 1$. For the tracking part, the sliding surface and the derived control law are chosen as

$$s(t) = ce_1(t) + \delta\int_0^\infty e_1(t)dt \tag{22}$$

$$u = \frac{1}{-L_g h(x)c}(cL_f h(x) + \delta \cdot e_1 + ks + \xi sat(s) + \mu s^{p/q}) \tag{23}$$

where the parameters c, δ, k, ξ and μ have a significant impact on tracking performance, which is optimized by PSO while $p = 5$, $q = 7$ and $\Delta = 0.05$ are fixed. ξ stands for the responsiveness to disturbances, δ is for the steady-state error, c, k, and μ are related to the tracking accuracy while the latter two also determine the finite time convergence. We would like to point out that compared to the general control law in Equation (7), the addition of c in Equation (22) provides more flexibility in the process of parameter tuning. For sure, we could simply make $c = 1$ for further optimization. Concerning the parameter setting in PSO, we choose the swarm size $m = 20$, the system dimension $l = 5$, the maximum number of iterations $G_{max} = 200$, the acceleration coefficients $C_1 = C_2 = 1.4$, the inertia weight bound $\mathbb{W} = [0.4, 0.9]$. Taking the tracking accuracy, robustness, and the desired finite time convergence into account, the bounds of parameters $k \in [1, 60]$, $\xi \in [1, 100]$, $\mu \in [0.01, 1]$, $c \in [0.1, 20]$, $\delta \in [0.001, 0.01]$ are set after few trials, the respective velocity is set as ten percent of the searching space accordingly. The fitness function is selected as the integral square error.

The parameters in the tracking controller are optimized and depicted in Figure 8.

Where we observe that $k = 42.02$, $\xi = 90.68$, $\mu = 0.89$, $c = 0.34$ and $\delta = 0.0013$ are finally determined for tracking control. Note that compared to the other parameters, the value of integral term δ is comparatively small such that its variation is not easily observable. To make Figure 8 concise, instead of using an amplified curve, the variation of δ is only described and marked by the key points that change in conjunction with other parameters. Also, the variations of fitness value and the linear time-varying inertia weight in Equation (13) are presented in Figure 8. In Figure 9, the control input, reference tracking, and the derived tracking error are presented.

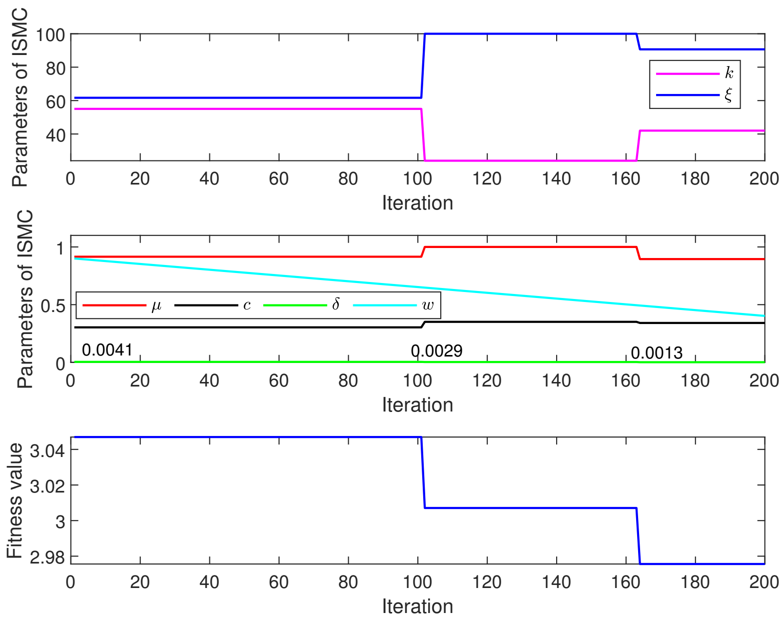

Figure 8. The variations of the optimized parameters with fitness value under PSO.

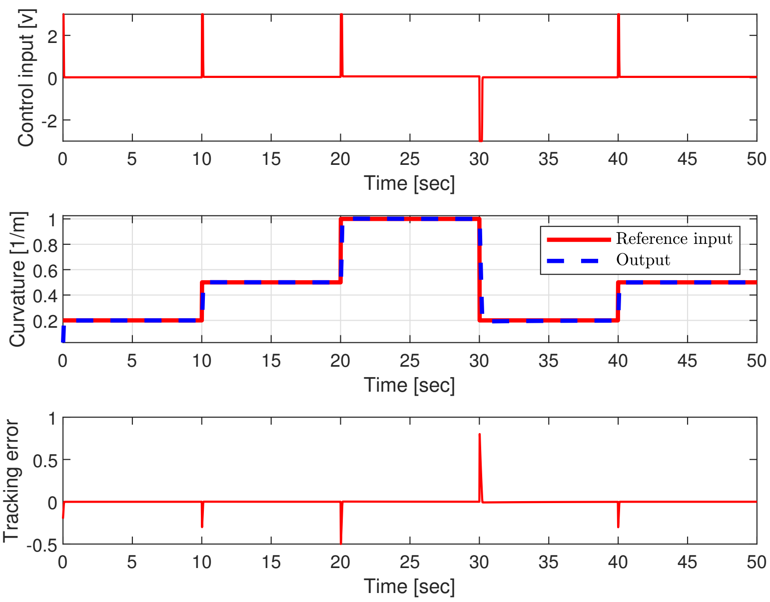

Figure 9. Accurate position tracking control with the ISMC−RRCF method.

It can be seen that the curvature of the highly nonlinear IPMC can be tracked by using the ISMC-RRCF method according to the time-varying reference. Also, in order to show the chattering effect on tracking, the results derived from ISMC with $sign(\cdot)$ are given in Figure 10, where it can be seen that the fast discontinuous switching control actions result in a decrease in tracking accuracy.

We would like to point out that although the chattering can be alleviated by the usage of the boundary layer method, the tracking performance may be significantly influenced by the inappropriate thickness of the boundary layer, which leads to tracking performance deterioration. The reason could be the fact that the thickness is too small to suppress the chattering while the larger ones are able to completely eliminate the chattering but at the expense of the reduction in robustness and tracking performance, cf., Figure 11.

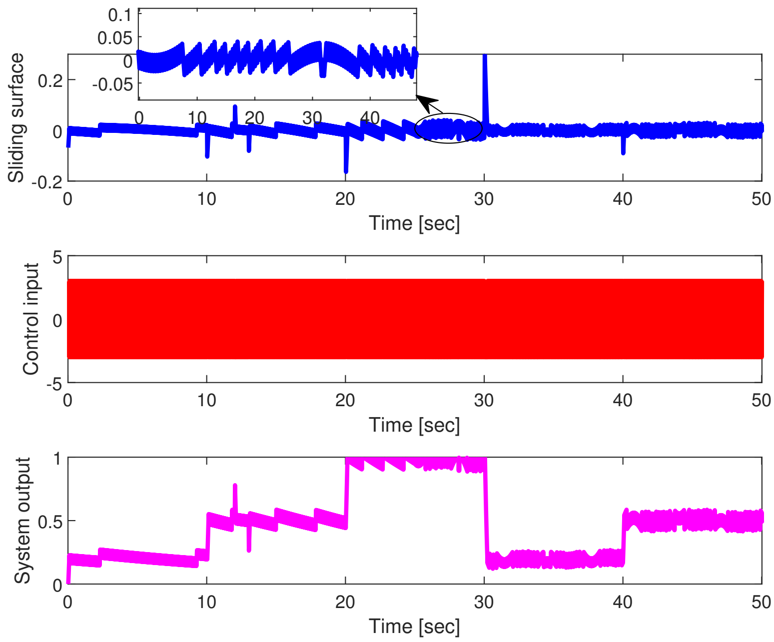

Figure 10. The control results derived by the ISMC method with $sign(\cdot)$ function.

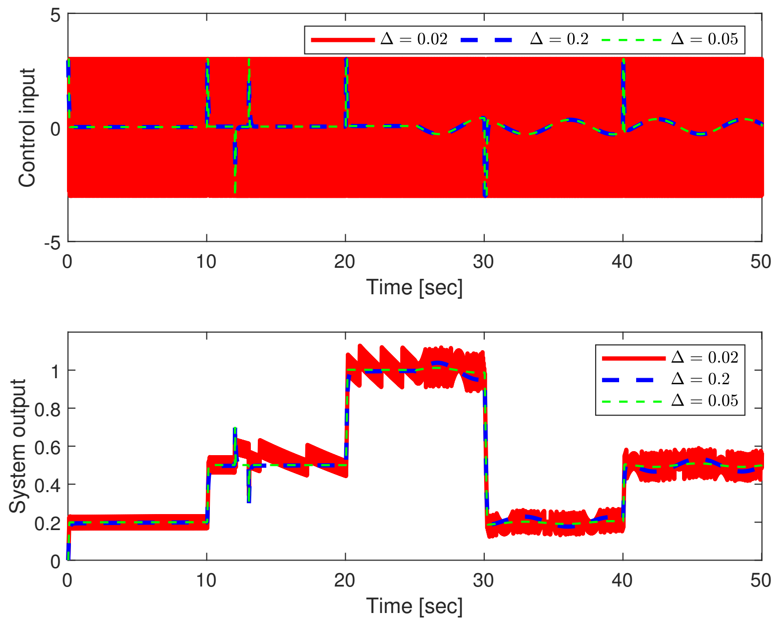

Figure 11. Different thickness of boundary layer for trajectory tracking.

In order to show the superiority of the proposed method in terms of tracking accuracy and robustness, we take the state-of-the-art methods including PID and PI-RRCF for comparison in the presence of model uncertainty and external disturbance. To this end, the external disturbance signal with $d = 0.2$ and the model uncertainty with $d = 0.02sin(t)$ are assumed and added when $t \in [12, 13]$ and $t \in [25, 50]$, respectively. In the upper side of Figure 12, we observe that the variations of control inputs for tracking are almost identical but the ISMC-RRCF has the fastest response to the external disturbance. On the downside, considering the model uncertainty, ISMC-RRCF has a better tracking accuracy compared to the other two methods.

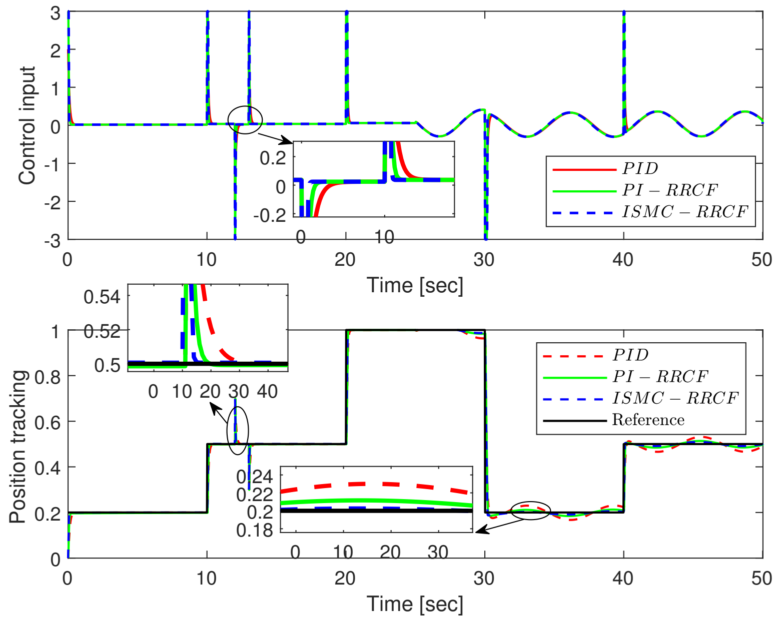

Figure 12. Comparison of different control methods for trajectory tracking in the presence of model uncertainty and external disturbance.

Also, according to the Equation (9) with the derived k, μ, q, p, and s_0, the finite time is obtained as $t_s = 0.2603$, which can be verified in Figure 13 in which the convergence time is less than t_s.

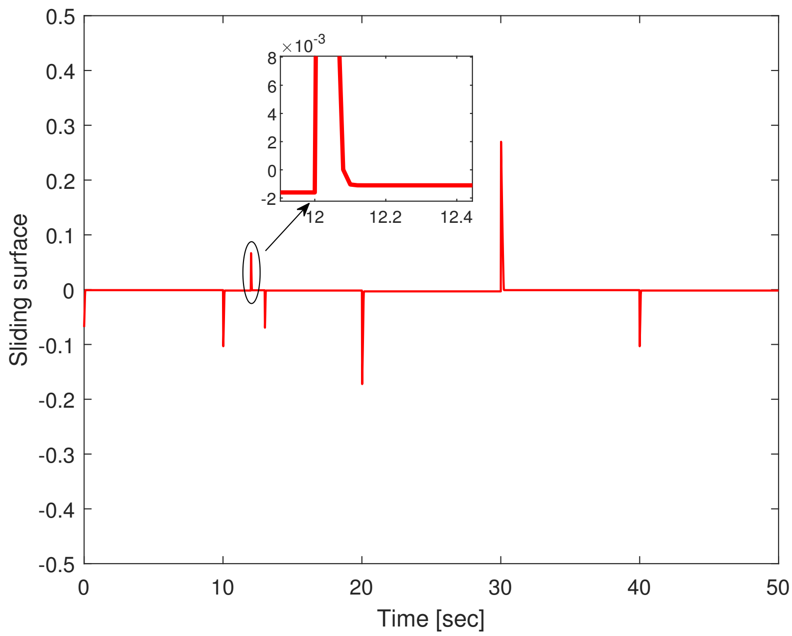

Figure 13. Finite time convergence of ISMC−RRCF in the presence of external disturbance.

6. Conclusions and Outlook

In this paper, we propose an intelligent ISMC-RRCF-PSO control method for the accurate trajectory tracking of a class of nonlinear systems in the presence of bounded model uncertainty and external disturbance. Utilizing the robust right coprime factorization method, the uncertain system plant can be decomposed as two stable operators and then the related controllers are designed for robust stability while meeting the Bezout identity. In order to improve the tracking performance, an ISMC law with finite time convergence is designed based on the method of Lyapunov stability analysis. The chattering with and without boundary layer methods are discussed and verified through extensive numerical simulations, and we conclude that the thickness is of significant importance to tracking accuracy. Further, the critical parameters of ISMC are optimized by the stabilizing PSO with linear time-varying inertia weight instead of manually tuning, which is time-consuming and without adaptability. The optimized parameters tuning is carried out by minimizing the cost function associated with the tracking error dynamics. Thereafter, the determined parameters are used for the ISMC-RRCF control to achieve the desired tracking performance. The proposed method is evaluated on a highly nonlinear IPMC application for the time-varying precise position tracking control. Compared with the state-of-the-art methods, the proposed method outperforms the PID and PI-RRCF methods in terms of tracking accuracy and quick reaction to disturbance.

In the future, the tracking performance may be further enhanced with the adaptive boundary layer method instead of using the fixed ones. Also, the basic PSO algorithm adopted in this paper for continuous optimization could be extended and improved such that the fitness function can be more flexible with certain constraints of control objectives.

Author Contributions: Conceptualization, P.L.; methodology, Q.Z. and P.L.; software, Q.Z. and J.P.; validation, Q.Z. and A.T.; writing—original draft preparation, Q.Z. and P.L.; writing—review and editing, Q.D. and J.P.; visualization, Q.Z. and Q.D.; supervision, P.L. All authors have read and agreed to the published version of the manuscript.

Funding: This research is partially supported by the National Natural Science Foundation of China (62202434, 62201510), the Key Scientific and Technological Project of Henan Province (232102220054, 222102210115, 232102220068, 232102221014, 222102210019), the High-end Foreign Expert Program of Henan Province (HNGD2023029), and the Scientific Research Team Plan of Zhengzhou University of Aeronautics (23ZHTD01001).

Data Availability Statement: The data presented in this study are available on request from the corresponding author.

Conflicts of Interest: The authors declare no conflict of interest.

References

1. Ang, K.H.; Chong, G.; Li, Y. PID control system analysis, design, and technology. *IEEE Trans. Control Syst. Technol.* **2005**, *13*, 559–576.
2. Kim, T.H.; Maruta, I.; Sugie, T. Robust PID controller tuning based on the constrained particle swarm optimization. *Automatica* **2008**, *44*, 1104–1110. [CrossRef]
3. Joseph, S.B.; Dada, E.G.; Abidemi, A.; Oyewola, D.O.; Khammas, B.M. Metaheuristic algorithms for PID controller parameters tuning: Review, approaches and open problems. *Heliyon* **2022**, *8*, e09399. [CrossRef]
4. Grüne, L.; Pannek, J. *Nonlinear Model Predictive Control: Theory and Algorithms, Communications and Control Engineering*; Springer: London, UK, 2017.
5. Zhang, Q.; Liu, P.; Pannek, J. Combining MPC and integer operators for capacity adjustment in job-shop systems with RMTs. *Int. J. Prod. Res.* **2019**, *57*, 2498–2513. [CrossRef]
6. Mayne, D.Q.; Kerrigan, E.C.; Van Wyk, E.J.; Falugi, P. Tube-based robust nonlinear model predictive control. *Int. J. Robust Nonlinear Control* **2011**, *21*, 1341–1353. [CrossRef]
7. Zhang, Q.; Liu, P.; Chen, Y.; Deng, Q.; Pannek, J. An improved event-triggered predictive control for capacity adjustment in reconfigurable job-shops. *Int. J. Prod. Res.* **2022**, *61*, 5974–5991. [CrossRef]
8. Deng, M.; Inoue, A.; Ishikawa, K. Operator-based nonlinear feedback control design using robust right coprime factorization. *IEEE Trans. Automat. Control* **2006**, *51*, 645–648. [CrossRef]
9. Deng, M. *Operator-Based Nonlinear Control Systems: Design and Applications*; John Wiley & Sons: Hoboken, NJ, USA, 2014.
10. Liu, P.; Zhang, Q.; Pannek, J. Development of operator theory in the capacity adjustment of job shop manufacturing systems. *Appl. Sci.* **2019**, *9*, 2249. [CrossRef]
11. Deng, M.; Wang, A. Robust non-linear control design to an ionic polymer metal composite with hysteresis using operator-based approach. *IET Control Theory Appl.* **2012**, *6*, 2667–2675. [CrossRef]

12. Liu, P.; Zhang, Q.; Wang, A.; Wen, S.; Pannek, J. Operator-Based Adaptive Tracking Capacity Control in Complex Manufacturing Processes. *Appl. Sci.* **2019**, *13*, 449. [CrossRef]
13. Dong, G.; Deng, M. Operator-Based Fractional-Order Nonlinear Robust Control for the Spiral Heat Exchanger Identified by Particle Swarm Optimization. *Electronics* **2022**, *11*, 2800. [CrossRef]
14. Huang, Y.J.; Kuo, T.C.; Chang, S.H. Adaptive sliding-mode control for nonlinear systems with uncertain parameters. *IEEE Trans. Syst. Man Cybern. B Cybern.* **2008**, *38*, 534–539. [CrossRef] [PubMed]
15. Gao, X.; Deng, M. Tracking performance improvement for operator-based nonlinear robust control of wireless power transfer systems with uncertainties. *Int. J. Control Autom. Syst.* **2019**, *17*, 545–554. [CrossRef]
16. Bu, N.; Liu, H.; Li, W. Robust passive tracking control for an uncertain soft actuator using robust right coprime factorization. *Int. J. Robust Nonlinear Control* **2021**, *31*, 6810–6825. [CrossRef]
17. Lee, H.; Utkin, V.I. Chattering suppression methods in sliding mode control systems. *Annu. Rev. Control* **2007**, *31*, 179–188. [CrossRef]
18. Fleming, P.J.; Purshouse, R.C. Evolutionary algorithms in control systems engineering: A survey. *Control Eng. Pract.* **2002**, *10*, 1223–1241. [CrossRef]
19. Tang, J.; Liu, G.; Pan, Q. A review on representative swarm intelligence algorithms for solving optimization problems: Applications and trends. *IEEE/CAA J. Automat. Sin.* **2021**, *8*, 1627–1643. [CrossRef]
20. Fakoor, M.; Nikpay, S.; Kalhor, A. On the ability of sliding mode and LQR controllers optimized with PSO in attitude control of a flexible 4-DOF satellite with time-varying payload. *Adv. Space Res.* **2021**, *67*, 334–349. [CrossRef]
21. Eltayeb, A.; Rahmat, M.F.; Basri, M.A.M.; Mahmoud, M.S. An improved design of integral sliding mode controller for chattering attenuation and trajectory tracking of the quadrotor UAV. *Arab. J. Sci. Eng.* **2020**, *45*, 6949–6961. [CrossRef]
22. Vahidi-Moghaddam, A.; Rajaei, A.; Ayati, M.; Vatankhah, R.; Hairi-Yazdi, M.R. Adaptive prescribed-time disturbance observer using nonsingular terminal sliding mode control: Extended Kalman filter and particle swarm optimization. *IET Control Theory Appl.* **2020**, *14*, 3301–3311. [CrossRef]
23. Chen, B.S.; Lee, C.H.; Chang, Y.C. H^∞ tracking design of uncertain nonlinear SISO systems: Adaptive fuzzy approach. *IEEE Trans. Fuzzy Syst.* **1996**, *4*, 32–43. [CrossRef]
24. Zhang, Q.; Liu, P.; Chen, Y.; Deng, Q.; Tong, A. Disturbance observer-based terminal sliding mode tracking vontrol for a class of nonlinear SISO systems with input saturation. *Processes* **2023**, *11*, 1878. [CrossRef]
25. Saha, S.; Amrr, S.M.; Saidi, A.S.; Banerjee, A.; Nabi, M. Finite-time adaptive higher-order SMC for the nonlinear five DOF active magnetic bearing system. *Electronics* **2021**, *10*, 1333. [CrossRef]
26. Kennedy, J.; Eberhart, R. Particle swarm optimization. In Proceedings of the ICNN'95—International Conference on Neural Networks, Perth, WA, Australia, 27 November–1 December 1995; Volume 4, pp. 1942–1948.
27. Zhang, Y.; Wang, S.; Ji, G. A comprehensive survey on particle swarm optimization algorithm and its applications. *Math. Probl. Eng.* **2015**, *2015*, 931256. [CrossRef]
28. Nickabadi, A.; Ebadzadeh, M.M.; Safabakhsh, R. A novel particle swarm optimization algorithm with adaptive inertia weight. *Appl. Soft Comput.* **2011**, *11*, 3658–3670. [CrossRef]
29. Gopal, A.; Sultani, M.M.; Bansal, J.C. On stability analysis of particle swarm optimization algorithm. *Arab. J. Sci. Eng.* **2020**, *45*, 2385–2394. [CrossRef]
30. Aabloo, A.; Belikov, J.; Kaparin, V.; Kotta, Ü. Challenges and perspectives in control of ionic polymer-metal composite (IPMC) actuators: A survey. *IEEE Access* **2022**, *8*, 121059–121073. [CrossRef]